Improving of hot forging tool life hardfaced by Stellite-6

W. FEKIH AHMED[a], H. BONNEFOY[a], P. REVEL[b], A. LODINI[a]

[a] Laboratoire d'Analyse des Contraintes Mécaniques et de Dynamique des Transferts aux Interfaces LACMDTI, Université de Reims UFR science, Moulin de la housse 5100 Reims, FRANCE.
[b] Laboratoire Roberval, UMR 6253, UTC/CNRS, Centre de Recherches de Royallieu, BP 20529, 60205 Compiègne, France.

Abstract: Hot forging tools are subjected to high cyclic thermo-mechanical stresses resulting in their premature failure. Forging materials such as stainless steels and titanium alloys accelerates the degradation of these tools. The aim of this study is to improve lifetime of hot forging tools using thick hardfacing. The retained solution is a cobalt base (Stellite-6) hardfacing deposited by PTA (Plasma Transferred Arc) process. Cobalt base alloys are attractive owing to an excellent corrosion resistance and a good resistance to thermal fatigue over a wide temperature range. PTA deposition allows to obtain very interesting characteristics of coating such as a strong metallurgical bond to the substrate, a low dilution and homogeneous refined microstructure of coating. Isothermal low cycle fatigue tests were performed on cylindrical specimens machined in substrate and coating in the temperature range of tool service (20-700°C). Determination of coating mechanical behaviour and comparison of isothermal fatigue behaviour with tool steel are presented. Microstructural analyses were performed in order to highlight failure mode of cobalt base coating. A viscoplastic kinematic and isotropic hardening model was chosen in order to determine and simulate thermo-mechanical stresses in hardfaced forging tools. A hardfaced punch submitted to thermal cycling was tested in industrial condition. The results show that the use of Stelite-6 coating allows increasing by three the lifetime compared to a non hardfaced tool.

1 INTRODUCTION

Forging consists of plastic deformation process in which a metal billet or blank is shaped by tools or dies. Hot forging occurs at temperature of about $0.7T_L$ (Liquidus Temperature) [1]. Generally, due to forging billet temperature being well above 1000°C, the surface temperature of the tool temporarily exceeds 500°C [2-4]. Hot forging process involves three stages. The first stage is the brutal setting up of the billet with the die. The second stage is the metal forming during which the applied stresses to the tool are important. The third one is the part ejection and the tool cooling. This cycle, repeated thousand times, damages the hot forging tool. The nature of the damage is related to the geometry of the tool and the resulted thermomechanical stresses.

In order to increase the hot forging lifetime, the blacksmith use frequently surface treatments such as nitriding, hard chromium plating, preventive and repair hardfacing and more recently duplex treatment which combines gas nitriding followed by PVD coatings [5]. In our study, PTA (Plasma Transferred Arc) welding process which presents a very good alternative to other surface welding processes such as conventional techniques (shielded metal arc welding, gas metal arc welding, gas tungsten arc welding, submerged arc welding) or more recent ones such as laser cladding was selected[6]. In fact, this process allows to provide very interesting characteristics of coating such as low heat affected zone, low dilution levels, homogeneous refined microstructure and strong metallurgical bond to the substrate. This process allows also the deposition of a wide choice of metal powders, among them cobalt base superalloys. Stellite-6 is a Co-Cr-W-C alloy, which belongs to the Stellite trademark name of commercial Co-base hardfacing alloys developed by E. Haynes. In Stellite-6 alloy, Cr provides oxidation and corrosion resistance, as well as strength by formation of carbides. The weld overlay coating is effective for hot work where the thermal and tribological conditions are too severe for classics steels.

In this study, improving the lifetime of a hot forging tool submitted to thermal fatigue using a coating of Stellite-6 deposed by PTA process was chosen. The modelling of the thermal fatigue due to successive forging steps and cooling periods during, which free thermal expansion is partially or completely constrained, was performed in order to quantify the damage, to deduce the lifetime and to optimize the choice and thickness of the coating.

2 EXPERIMENTAL PROCEDURE

2.1 Coating

The coating was performed by equipment consisting of a 6-axys robot (COMAU) supporting the die and a PTA torch fixed on vertical position, see Figure 1. This configuration provides a better supply of powder in the torch. In this study we have chose a Co-base superalloy (Stellite grade 6) which confers to the coating a high harness over a wide temperature range, a good thermal resistance and a thermal expansion coefficient close to the tool steel used as substrate. The used powder, obtained by atomisation, presents a spherical morphology of a size of about 100µm with a low dispersion, a slightly oxidized grain surface and a uniform chemical composition.

The tested coating, on Stellite-6 was carried out on blocks of X38CrMoV5 steel (AISI H11). These steel blocs were quenched and tempered in the same conditions of our industry partners, providing a hardness of 46 HRC. The chemical composition of the used powder and of the chosen steel is given in Table 1. To ensure a good quality of the coating, an L8 Taguchi experimental design was made to obtain the optimal configuration of the process parameters.
The micrography, Figure 2 (a), shows a dendritic structure of the obtained coating. The examinations carried out, using energy dispersive spectroscopy probes (Ultradry–THERMO FISHER) coupled with Scaning Electronic Microscope (SEM) on a sample of Stellite-6 coating deposed by PTA process, revealed a difference in concentration of chemical composition between dendritic and interdendritic zones. A semi-quantitative analysis which allows to calculate the percentage of the elements in each area, shows that the dendritic areas are rich in cobalt, while the interdendritic areas are riches in chromium, carbon and tungsten, which favours the formation of carbides. The different types of carbides were identified by X-ray diffraction (XRD) as: Cr_7C_3, $Cr_{23}C_6$ and Co_6W_6C, Figure 2 (b). The presence of carbides provides to the coating a high hardness. The Rockwell hardness measured on the Stellite-6 coating is 52 HRC.

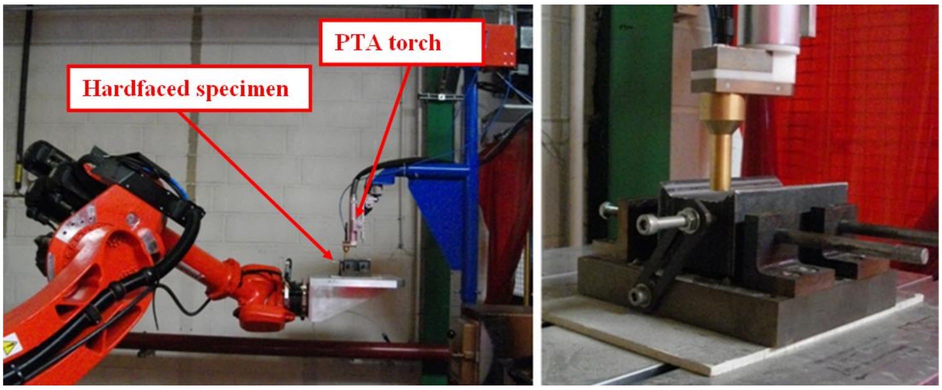

Figure 1. Hardfacing equipment: robot controller and PTA torch.

	C	Si	Mn	Mo	Cr	Ni	W	V	Co	Fe
X38CrMoV5	0,3 -0,5	0,3 -0,5	0,3 -0,5	2,7 -3,2	4,8 -5,2	-	-	0,4 -0,6	-	solde
Stellite 6	1,2	< 2	2	< 1	28,5	< 2	4,5	-	solde	< 2

Table 1. Chemical composition of Stellite-6 powder and X38CrMoV5 substrate (*wt%*).

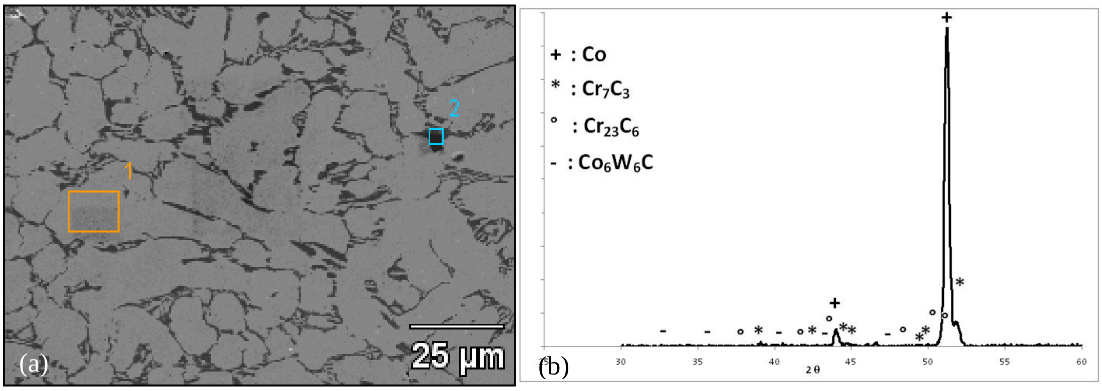

Figure 2. Micrograph showing the structure of Stellite-6 (a), X-ray diffraction pattern of Stellite-6 (b).

2.2 Study of the isothermal low cycle fatigue of the coating

The low cyclic fatigue tests were performed on a Mayes testing machine equipped with Joule effect furnace and a capacitive extensometer with ceramic rods that provide a 10 mm base. The tests were conducted at five temperature levels (20, 300, 500, 600 and 700°C). They were performed at two strain rates at $3.10^{-3}s^{-1}$ and $1.10^{-4}s^{-1}$ and at an imposed plastic strain. The first tests were performed at a strain rate of $3.10^{-3}s^{-1}$ and at three plastic strain amplitudes (±0.2, 0.5 and 1%). The second tests were conducted at constant plastic strain amplitude (± 0.5%) at two imposed strain rates at $3.10^{-3}s^{-}1$ and $1.10^{-4}s^{-1}$ followed by a relaxation. This experimental strategy was chosen to identify the parameters of the mechanical law and of the damage law. Only the results of first tests will be presented.
The used specimens were cut on parallel the direction of PTA deposition by electrical discharge machining in the form of bars of 12 mm in diameter and 100mm long and then machined using a numerically controlled turner. The specimens are then polished using emery paper with different grit 400, 800 and 1200 and then with a paste of alumina in order to obtain a mirror polished surface. The geometry specimen is defined by Figure 3 where the useful part is 12 mm long and 5 mm in diameter.

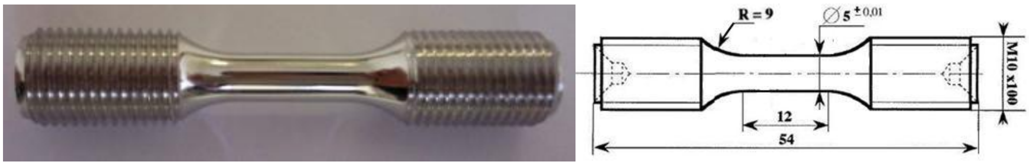

Figure 3. Low cycle fatigue test specimen.

2.3 Simulation of thermal fatigue of a hardfaced tool

The selected tool is a punch made from X38CrMoV5 employed to produce ball bearing race of 100Cr6. This tool is mainly submitted to thermal fatigue which aims to facilitate the numerical modelling of fatigue of tool. In this study, a Stellite-6 hardfacing was carried out on the punch by PTA process in 2 layers of 2 mm. The final thickness of coating after numerical controlled machining is about 2 mm, see Figure 4. A preheating operation is performed before the start of production of the punch at a temperature of about 250°C to avoid thermal shock.
In order to calculate the thermomechanical stresses in the hardfaced punch, a numerical simulation of five forging operations was carried out under the software Abaqus. An axisymmetric model was used in order to reduce the computation time. The mesh of the punch is performed by quadratic triangular elements (CAX6MT) used of thermomechanical modelling and adapted to the axisymmetric cases.
The mesh is refined for coating zone and for the substrate zone, which is close to the coating of a thickness of 4 mm. These zones correspond to the high gradient of temperature, Figure 5. The mechanical behavior parameters of both materials X38CrMoV5 and Stellite-6 have been identified and assigned respectively to the substrate and coating through an subroutine UMAT. The visoplastic used model is given by the constitutive equations as shown below.
The cycle time and the heat transfer coefficients were derived from a previous simulation carried out in the forge code (Forge 3). The simulation results of Forge 3 have confirmed that the type of stresses is essentially thermo-mechanical due to the high gradient of temperature located near the contact surface of the punch.

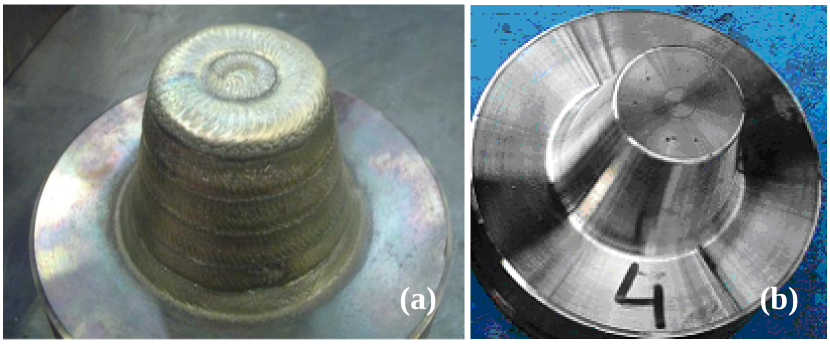

Figure 4. Punch with PTA Stellite-6 deposit (a), before forging (b).

Constitutive equations of used model:

- Total strain partition: $\underline{\varepsilon} = \underline{\varepsilon}^{el} + \underline{\varepsilon}^{pl} + \underline{\varepsilon}^{th}$ (1)
- Generalized Hooke's law: $\underline{\sigma} = \lambda tr\left(\underline{\varepsilon}^{el}\right) I + 2\mu\underline{\varepsilon}^{el}$ (2)
- Flow rule for the inelastic strain: $\dot{\underline{\varepsilon}}^{pl} = \dot{p} = \left\langle \frac{f}{K} \right\rangle^{n}$ $with: f = \left|\underline{\sigma} - \underline{X}\right| - R - \sigma_y$ (3)
- Isotopic hardening: $R = Q\left(1 - e^{(-bp)}\right)$ (4)
- Kinematic hardening: $\dot{\underline{X}} = C_1\dot{\underline{\alpha}} + C_2\dot{\underline{\varepsilon}}^{pl}$ (5)
- Internal variable for kinematic hardening: $\dot{\underline{\alpha}} = \dot{\underline{\varepsilon}}^{pl} - \gamma(p)\dot{p}\underline{\alpha}$ (6)

With: $\gamma(p) = \gamma_s + \left(\gamma_0 - \gamma_s\right)e^{(-\beta p)}$ (7)

Ten parameters characterize viscoplasticity:

- K, n : viscosity parameters
- σ_y : Initial threshold stress
- Q, b : Isotropic hardening parameters
- $C_1, C_2, \gamma_0, \gamma_s, \beta$: Kinematic hardening parameters

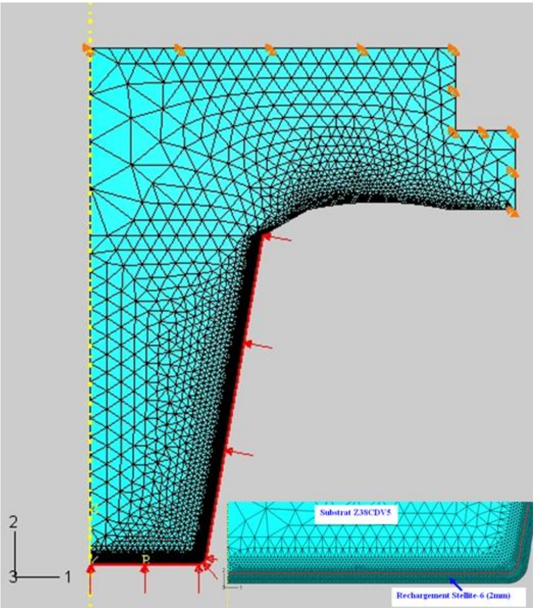

Figure 5. Finite element mesh of coated punch.

3 RESULTATS

3.1 Isothermal low cycle fatigue tests

The results of isothermal low cycle fatigue tests carried out for imposed plastic strain ±0.5% and for strain rate of $3.10^{-3}s^{-1}$ at various temperatures are shown in Figure 6. The evolution of semi-stress amplitude $\Delta\sigma/2$ with respect of accumulated plastic strain $\bar{\varepsilon}^{pl}$ shows that at room temperature a cyclic softening occurs. Whereas, for temperature range from 300°C to 700°C the semi-stress amplitude increase rapidly before it stabilizes, *i.e.* a cyclic hardening occurs.

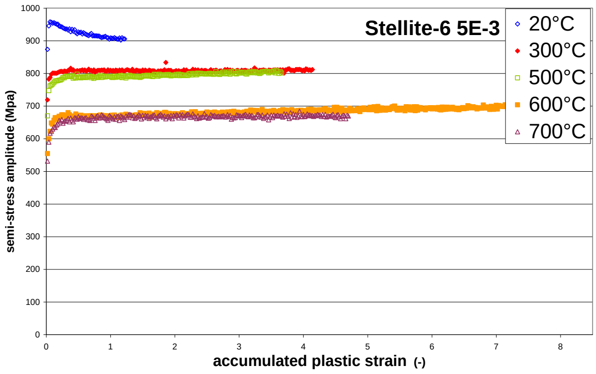

Figure 6. Evolution of $\frac{\Delta\sigma}{2}$ as a function of $\bar{\varepsilon}^{pl}$ at different temperatures; fatigue test of Stellite-6 at $\frac{\Delta\varepsilon^{pl}}{2} = 0.5\%$.

The fatigue life of Stellite-6, studied at various temperatures, is plotted in the classical Manson-Coffin diagrams as a function of plastic strain amplitude, Figure 7. The relationship of imposed plastic strain $\Delta\varepsilon^{pl}$ and the number of cycle to fracture N_R strongly depends of test temperature. The highest fatigue life is at 500°C and for low imposed plastic strain (0.2%). The Manson-Coffin curves were established and the fatigue life parameters (C, $\gamma+1$) were obtained via least square minimising procedure as shown in Table 2. The high parameters variation depending on temperature does not allow the approach of non-isothermal fatigue cases.

- The Manson-Coffin law: $$N_R = \left(\frac{\Delta\varepsilon^{pl}}{C}\right)^{-(\gamma+1)}$$

With: $\Delta\varepsilon^{pl}$: plastic strain amplitude
N_R : the number of cycle to fracture

The observations on fracture surface of fatigue specimens carried out using SEM have not revealed the initiation fatigue zone for all tested specimens. The Figure 8 represents a global view example of fracture surface. A predominantly brittle fracture is observed, which characterized by the presence of cleavage zones. A numerous spherical micro-cavities were also observed in some zones which indicate the presence of ductile fracture, Figure 8 (a). A more precise analysis using energy dispersive X-ray analysis system (EDS) on SEM were carried out on ductile fracture and brittle fracture zones have revealed that brittle fracture zone is richer in chromium and poorer in cobalt than ductile fracture zone. The comparison of theses results with the results of composition analysis of dentritic and interdentritic zones means that the brittle fracture is localised in interdentritic zones while ductile fracture is localised in dentritic zones.

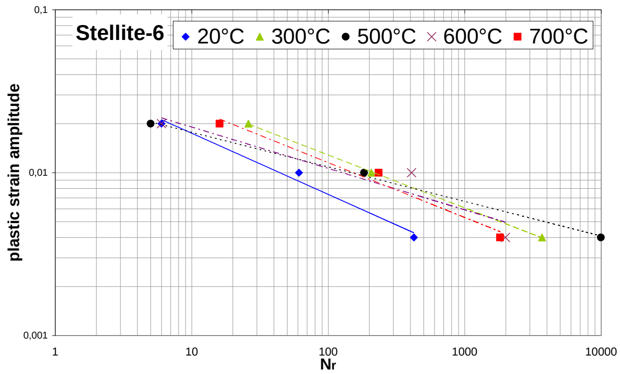

Figure 7. Fatigue life N_r as a function of plastic strain amplitude $\Delta\varepsilon^{pl}$ at different temperatures.

$N_R = \left(\frac{\Delta\varepsilon^{pl}}{C}\right)^{-(\gamma+1)}$	$\gamma+1$	C
20°C	2,62	$4,2610^{-2}$
300°C	3,08	$5,7210^{-2}$
500°C	4,70	$2,8910^{-2}$
600°C	3,51	$4,0310^{-2}$
700°C	2,90	$5,6310^{-2}$

Table 2. The Manson-Coffin parameters of Stellite-6.

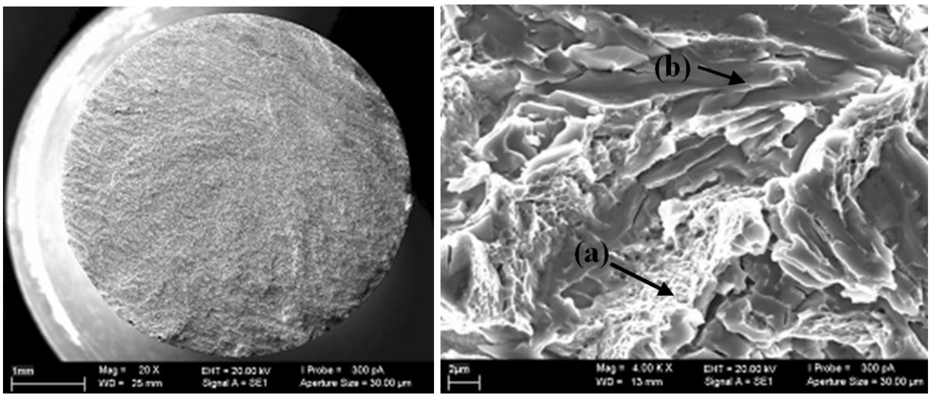

Figure 8. Micrographs of fracture surface of fatigue specimen: (a) ductile fracture zone and (b) brittle fracture zone.

The comparison of the isothermal low cycle fatigue test results between Stellite-6 and the quenched and tempered X38CrMoV5 tool steel is shown in Figure 9. This comparison shows that at room temperature, the Co-base hardfacing fatigue life is lower than that of tool steel whatever the imposed plastic strain. However, from 300°C and for low imposed plastic strain, the Co-base hardfacing fatigue life is much higher than that of tool steel. This result is very interesting because the hot forging tools are submitted to low cycle thermal fatigue during which the level of plastic strain per cycle of tool is very low which corresponds to last cases.

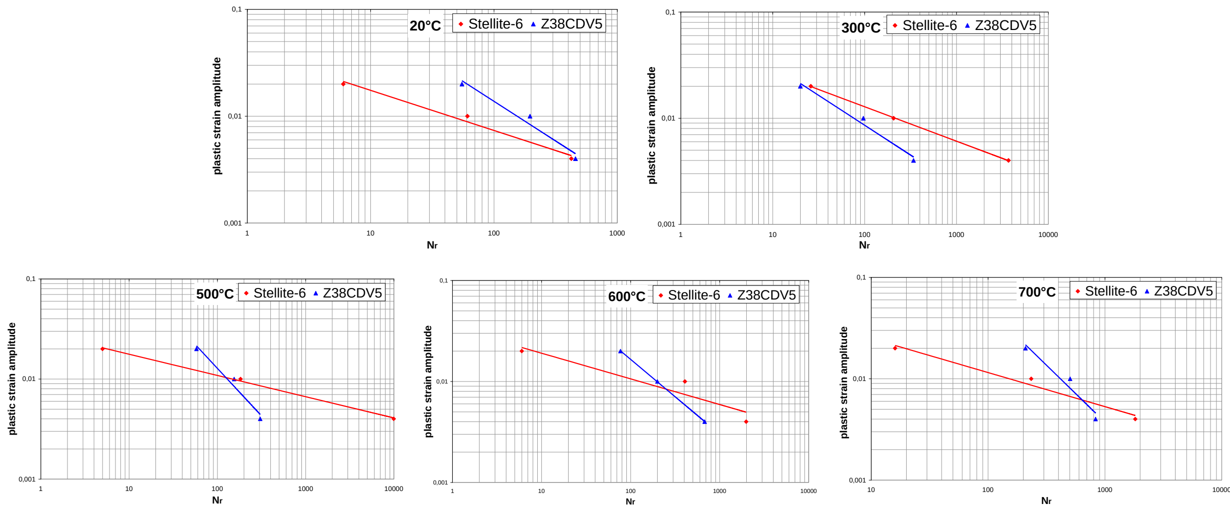

Figure 9. Comparison of fatigue life between Stellite-6 coating and X38CrMoV5 steel at different temperatures.

3.2 Thermal fatigue of hardfaced tool

The evolution of temperature with time and at different depths relative to thermal cycling is shown in Figure 10. A strong temperature gradient occurs in the coating zone. A temperature decrease of 300°C is located in a depth of 0.5 mm. The evolution of the stress versus time and depth is shown in Figure 11. During the heating phase that corresponds to the forging operation, the thermal expansion of the coating surface is partially constrained generate compression stress. During the cooling phase, temperature decreases faster at the surface of coating, which generate tension stresses. Moreover, the stress amplitude level decreases in function of depth. After five cycles the stress is in tension at surface and exceeds 400MPa, while in the substrate the stress is in compression. Figure 12 shows the evolution of accumulated plastic strain at the coating surface and at a depth of 0.5 mm. This result indicates that the plastic strain occurs significantly at the surface of coating. This accumulated plastic strain leads to cumulative fatigue damage.

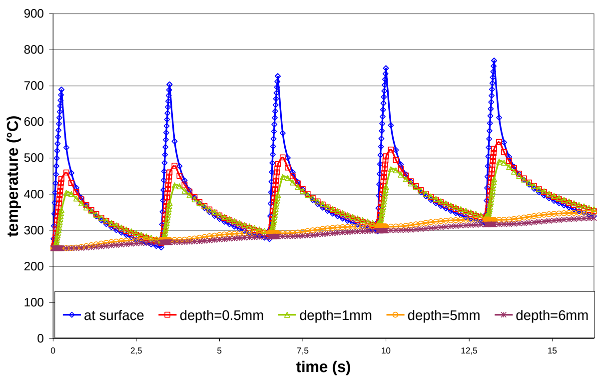

Figure 10. Evolution of temperature as a function of time at different depths.

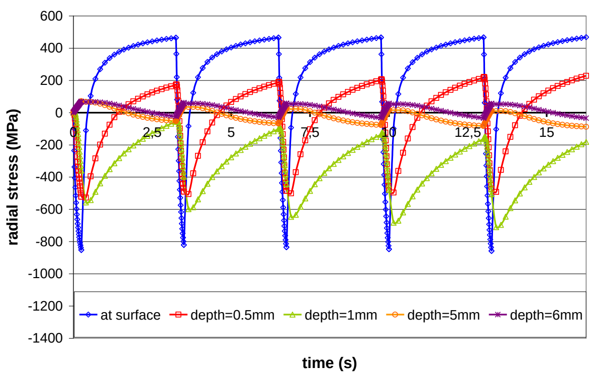

Figure 11. Evolution of radial stress σ_{rr} as a function of time at different depths.

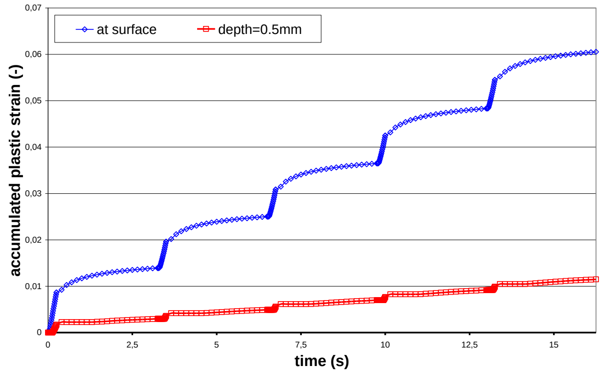

Figure 12. Evolution of accumulated plastic strain versus time at the surface of coating and at a depth of 0.5 mm.

The residual stresses evaluation was performed by ultrasonic technique on the damaged punch after forging cycles. Ultrasonic techniques for measurement of stress are based on the acousto-elastic effect, which correlates the stress field in a material with changes in the ultrasonic wave speed [8-10]. The critically refracted longitudinal wave is more sensitive to stress and less sensitive to the texture of the material, hence the choice of this technique. The measurements at different frequencies (1, 2, 3, 5 MHz) were allowed to evaluate the stress at different depths.

The numerical simulation results shown a good agreement with the residual stresses measured by ultrasonic technique, Figure 13. The differences may be caused by compressive stresses due to the hardfacing process, despite the tool tempering at 550°C.

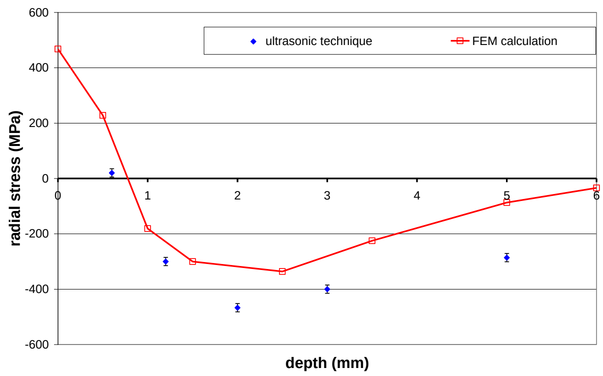

Figure 13. Results of residual stress σ_{rr} at different depths obtained by ultrasonic technique measure and FEA calculation.

Figure 14 shows the status of the punch in the end of life. A network cracks on coating surface characteristic of thermal fatigue is visible on the front face of the punch. The use of Stellite-6 weld overlay coating on the punch has tripled production, compared to the uncoated punch, to reach 3000 parts.

Vickers hardness measurements were carried out on the coating surface of punch on five points, before forging and at the end of service as shown in Table 3. The increase of coating hardness can be correlated to the cyclic strain hardening undergone by the punch surface during the forging cycles.

XRD analysis was performed on the front face of the punch at the end of service. The result of this analysis reveals that no change of phase appear especially the transformation of Co-γ → Co-ε, which risks to deteriorate tool life [11-12].

Figure 14. Hardfaced punch after forging cycles.

HV30	Measurement n°1	Measurement n°2	Measurement n°3	Measurement n°4	Measurement n°5	Average	Standard deviation
Before forging cycles	429	437	429	404	400	420	16,6
After forging cycles	481	478	473	481	490	481	6,18

Table 3. Measures of coating surface hardness before and after forging cycles.

4 CONCLUSIONS

The use of superalloys hardfacing presents an efficient solution to increase the hot forging tool life, which requires the optimisation of the coating thickness and used material. Isothermal low cyclic fatigue tests were carried out in order to identify mechanical behavior and fatigue law parameters of co-base hardfacing and tool steel, which allows the numerical simulation of the thermal fatigue and the damage of hardfaced tool. The isothermal low cyclic fatigue tests revealed that at room temperature the fatigue life of coating is lower than that of tool steel. However, from 300°C the fatigue life of coating is much higher than that of tool steel at low imposed plastic strain, which corresponds to tool strain during forging service.

The study of an industrial case of a punch hardfaced has conducted that the use of Stellite-6 hardfacing deposited by PTA had a beneficial effect on the lifetime of the punch, which has increased by three times.

Numerical simulation of thermal loading undergone by the punch shows a good agreement between the simulation result and the residual stresses measured by ultrasonic technique. Further analysis of the punch at the end of life revealed a thermal fatigue and hard cycling of the coating. Taking into account the phenomenon of thermal cycling is justified under the state of the punch at the end of service. The thermal cycling generates an increase of hardness of coating, which is due to hard cycling.

The parameters of the damage law depend strongly on temperature of tests. This makes the application of this damage law of impossible in the case of non isothermal loading especially the thermal cycling. Other approaches based on the reduced stress should be explored to overcome the dependence of parameters to temperature.

5 ACKNOWLEDGEMENTS

The authors would like to thanks very much the ANR (French National Research Agency) for it financial support for this study and the Ardennes forging companies, our project partners for their collaboration and availability.

6 REFERENCES

1- Metalworking: Bulk Forming, ASM Handbook, Volume 14A, 2005.
2- G. Andreis, K. D. Fuchs, I. Schruff, The wear behaviour of hot-work tool steels used in forging processes, in Proceedings of the 5th International Conference on Tooling , Loeben, 1999, 593-600.
3- S. Walter, H. Haferkamp, M. Niemeyer, Fr. W. Bach, A. Henze, Material failure mechanisms of forging dies, in Proceedings of the 5th International Conference on Tooloing, Loeben, 1999, 215-224.
4- D. Kircher, PhD thesis, Université de Reims Champagne-Ardenne, 1999.
5- J. Smolik, M. Gulde, J. Walkowicz, J. Suchanek, Influence de la structure du composite : couche nitrurée/revêtement PVD sur la durabilité des matrices de forgeage en acier DIN-1.2367, Surface et coatings technology, 2004.
6- A.S.C.M. d'Oliveira, R. Vilar, C.G. Feder, Applied Surface Science 201, 2002, 154 –160.
7- J.L. Chaboche, Constitutive equations for cyclic plasticity and cyclic viscoplasticity, International Journal of Plasticity 5, 1989, 247-302.
8- F. Belahcene, Détermination des contraintes résiduelles par méthode ultrasonore, Techniques de l'Ingénieur, 2002.
9- M. Ya, P. Marquette, F. Belahcene, J. Lu, Residual stresses in laser welded aluminium plate by use of ultrasonic and optical methods, Materials Science and Engineering A 382, 2004, 257–264.
10- D. Murnachan , Finite deformation of an elastic solid, John Willey, 1951, New York.
11- R.G. Barrows, J.B. Newkirk, Phase equilibria in the Co–Cr–W system with special emphasis on the R-phase, Metallography 5, 1972, 515–541.
12- L. Bourithis, V. Gontzes, G.D. Papadimitriou, Failure analysis of stellite dies for brass extrusion: The effect of aging, Journal of Materials Processing Technology 182, 2007, 608–614.